Kinetics of Liquid-Phase Hydrogenation of Isooctenes on a Pd/γ-Alumina Catalyst

Amitava Sarkar, Deepyaman Seth, Flora T. T. Ng, and Garry L. Rempel
Dept. of Chemical Engineering, University of Waterloo, Waterloo, Ontario, N2L 3G1 Canada

DOI 10.1002/aic.10722
Published online November 4, 2005 in Wiley InterScience (www.interscience.wiley.com).

The kinetics of liquid-phase hydrogenation of isooctenes [2,4,4-trimethyl-1-pentene (1-TMP) and 2,4,4-trimethyl-2-pentene (2-TMP)] was studied on a Pd/γ-Al_2O_3 catalyst in a semibatch reactor. Experimental results revealed that palladium was highly active for the hydrogenation of isooctenes and did not show any significant deactivation like that of the nickel, cobalt, or platinum catalysts reported in the literature. The internal double bond of 2-TMP was hydrogenated faster than the terminal double bond of 1-TMP. In addition to the hydrogenation reactions, double-bond isomerization was observed between 1-TMP and 2-TMP. A kinetic model was developed based on the Horiuti–Polanyi mechanism, involving a half-hydrogenated surface intermediate and the rate-limiting step was the first hydrogen addition. Isomerization was assumed to take place via the partly hydrogenated intermediates because no isomerization was observed in the absence of hydrogen. The dynamic reactor model consisted of material balances for the gas and the liquid phases, as well as for the porous catalyst particles. A resulting coupled ordinary differential equation–partial differential equation system was solved by Newton's method simultaneously with the minimization of the objective function from the kinetic model. The estimated model parameters with 95% confidence intervals accurately described the experimental data. The hydrogenation of both isomers was found to be strongly dependent on internal diffusion inside the catalyst particle. © 2005 American Institute of Chemical Engineers *AIChE J,* 52: 1142–1156, 2006

Keywords: liquid-phase hydrogenation, isooctenes, semibatch reactor, palladium/alumina, dynamic model

Introduction

Environmental restrictions regarding the use of methyl tertiary butyl ether (MTBE) have inspired refiners to search for new high-octane gasoline components.[1,2] Isooctane [2,2,4-trimethylpentane (TMPA)], the reference compound for measurement of the octane number of gasoline, can be a cost-effective replacement for the volume and octane number of MTBE in gasoline. TMPA has both a motor octane number (MON) and a research octane number (RON) of 100, which are higher than the typical octane ratings of commercially produced alkylates. A new process technology for isooctane production can be based on the utilization of the surplus isobutene from MTBE phase-out. Selective dimerization of isobutene results in isooctenes [2,4,4-trimethyl-1-pentene (1-TMP) and 2,4,4-trimethyl-2-pentene (2-TMP)]. Catalytic hydrogenation of isooctenes produces TMPA, which has a higher octane rating than that of isooctenes. Some commercial process configurations for isooctane units have been introduced.[3,4]

Although the selective dimerization of isobutene and subsequent in situ hydrogenation of isooctenes can simultaneously be performed in a single catalytic distillation (CD) reactor by exploiting the various advantages associated with CD technology,[5] no such process has yet been commercialized. Oligomerization of isobutene is an exothermic reaction[2] and the heat of reaction can be used for the distillation process. Instantaneous

Correspondence concerning this article should be addressed to F. T. T. Ng at fttng@cape.uwaterloo.ca.

Table 1. Summary of Reaction Conditions and Levels of Independent Variables Studied Experimentally in the Liquid-Phase Hydrogenation of Isooctenes in a Semibatch Reactor

Initial reactant	(1) Pure 1-TMP (3.5–8.5 mol %) in isopentane (2) Pure 2-TMP (5.5 mol %) in isopentane (3) Equilibrium mixture of 1-TMP (8.9 mol %) and 2-TMP (2.4 mol %) in isopentane
Temperature, °C	70, 80, 90, 100, 110, 120, 130
System pressure, kPa	963, 1136, 1308, 1480, 2170, 2860
Stirring speed, rpm	300, 500, 700

separation of products from the reaction mixture results in higher isobutene conversion and subsequent hydrogenation results in higher dimer selectivity by minimizing higher oligomer formation.

Detailed kinetic information on the hydrogenation of isooctenes is required for successful development and optimization of a CD-based isooctane process. The activity of the hydrogenation catalyst in a CD column reactor should be high enough to achieve almost complete hydrogenation of isooctene; otherwise, the octane number of the final product would be <100. The kinetics of hydrogenation of isooctenes on commercial catalysts such as Ni/Al_2O_3, Co/SiO_2, and Pt/Al_2O_3 has been reported.[6-8] Severe catalyst deactivation through the formation of carbonaceous deposits was observed when Pt/Al_2O_3 catalysts were used. The maximum conversion of isooctenes on Ni/Al_2O_3 catalyst under the conditions studied was 45% and the activity of the Co/SiO_2 catalyst was found to be considerably lower than that of the Ni/Al_2O_3 catalyst.[7] Although catalyst deactivation during the experiments was observed for all the catalysts mentioned above, Ni/Al_2O_3 showed the highest activity with the least deactivation by coke deposition. However, nickel catalysts have a very low resistance toward deactivation by sulfur and nitrogen compounds.[9] For the liquid-phase hydrogenation of isooctenes, it has been suggested that for feeds with >1 ppm of sulfur compounds, a noble metal catalyst should be used.[10]

Supported noble metal catalysts usually promote double-bond hydrogenation. The activity of a supported noble metal catalyst depends on the nature of olefin as well as on the nature of support. It is found that Pt is the most active catalyst for the hydrogenation of ethene and one of the least active catalysts for the hydrogenation of propene.[11] Generally for a given olefin, the ease of hydrogenation over supported noble metal catalysts decreases in the order: Pd ≥ Rh > Pt ≥ Ni ≫ Ru.[12,13] Palladium has the advantage of being the cheapest among the noble metals and has been used extensively for mechanistic studies. Supported Pd catalysts are relatively easy to prepare and have a high tolerance to resist poisoning and deactivation.[14] Therefore a supported palladium catalyst has the potential of being a very effective hydrogenation catalyst for a CD-based isooctane process.

The purpose of the present research was to determine the intrinsic kinetics of hydrogenation of isooctenes on a Pd/γ-Al_2O_3 catalyst and to establish the effect of isomerization between 1-TMP and 2-TMP on the hydrogenation reaction. The kinetics of liquid-phase hydrogenation of isooctenes was studied in a batch autoclave operated in a semibatch mode. It has been reported that the molar ratio of 1-TMP and 2-TMP in an isooctene mixture has an equilibrium molar composition ratio of approximately 4:1 over the temperature range of 50–100°C, which shifts slightly toward 2-TMP as the temperature is increased.[15] Given that the thermodynamic equilibrium between 1-TMP and 2-TMP is known, the kinetics of hydrogenation of the two isomers and the rate of their isomerization during hydrogenation can be determined by using a mixture of two isomers deviating from the equilibrium compositions as reactants. This information can then be used in the process development of a CD-based isooctane unit.

Experimental

Materials

An in-house Pd/γ-alumina catalyst (Pd loading, 0.72 wt %; specific surface area, 204 $m^2\ g^{-1}$; total Hg pore volume, 0.55 $cm^3\ g^{-1}$; bulk density, 618 kg m^{-3}) was used in all the experiments. Analytical-grade 2,4,4-trimethyl-1-pentene (T78409, 99%, Sigma–Aldrich, St. Louis, MO) and 2,4,4-trimethyl-2-pentene (143820, 99%, Sigma–Aldrich) were used as reactants and HPLC-grade 2-methylbutane (270342, 99.5+%, Sigma–Aldrich) was used as a solvent. Oxygen-free hydrogen (99.99+%), oxygen-free nitrogen (99.5+%), and oxygen-free argon (99.95+%) gases were supplied by Praxair Canada Inc. (Mississauga, Ontario) and used as received.

Methods

Before each experiment, the required amount of catalyst was calcined in air at 350°C for 4 h and then reduced under a constant flow of hydrogen (flow rate = 50 mL min^{-1}) at 350°C for 4 h. The prepared catalyst, stored in *n*-heptane under an argon atmosphere, was then transferred inside a glove bag under an argon environment to the "catalyst addition basket" of the reactor. The reactor was then sealed within the glove bag and purged with argon. After removing the reactor from the glove bag, the reactor was purged with hydrogen and the necessary connections were made. A mixture containing the required amount of 1-TMP and/or 2-TMP in 2-methylbutane (isopentane) was prepared in a closed tank and oxygen-free nitrogen was bubbled through the liquid mixture for 4 h through a dip tube, under constant stirring at 100 rpm, to remove any traces of dissolved oxygen. The tank was then kept pressurized to 50 psig with nitrogen.

The hydrogenation experiments were carried out over a wide range of reaction conditions, which are summarized in Table 1. All the experiments were performed in an SS 316 300 mL Parr autoclave operated in semibatch mode under constant hydrogen pressure (±5 kPa). The reactor was equipped with a magnetic stirrer, internal water cooling coil, a dip tube for liquid-phase sampling, and a dual-action programmable temperature controller (±1°C). A simplified schematic of the reactor setup is presented in Figure 1. The reactants were transferred from the preparation tank to the reactor with the help of a sampling

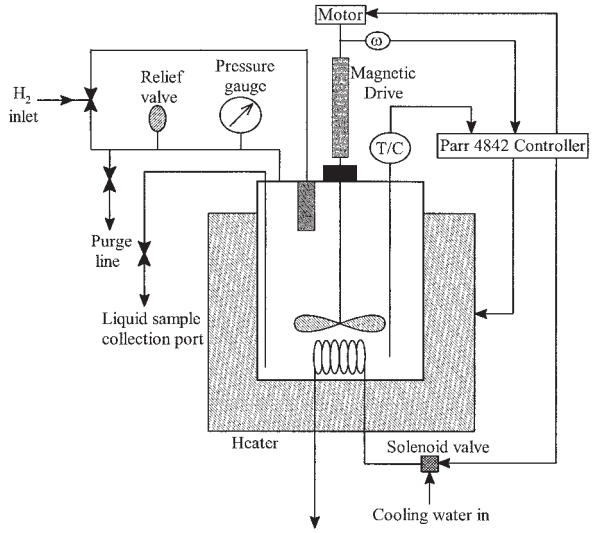

Figure 1. Experimental setup for liquid-phase hydrogenation of isooctenes.

bomb. The reactor, loaded with catalyst and reactant mixture, was set to the desired reaction temperature under constant stirring and pressurized with hydrogen to the desired reaction pressure. Sufficient time (1 h) was allowed for hydrogen to dissolve in the liquid phase at the desired reaction temperature and pressure. The catalyst was dropped into the reactor by a sudden increase of pressure in the line where the catalyst basket was attached. This pressure fluctuation did not, however, affect the pressure in the reactor because the volume of this line was very small compared to the vapor space volume of the reactor. The start of the reaction time was noted at the point when the catalyst was dropped into the reaction mixture. Liquid samples were collected during the reaction in an air-tight copper sampler and a gas-tight syringe was used for further handling. The samples were analyzed with a Agilent 6890 Series II GC system equipped with an HP-5 capillary column (length = 30 m; diameter = 0.32 mm; film thickness = 0.25; J&W Scientific, Agilent Technologies, Palo Alto, CA) and a flame ionization detector. Integration of the GC results was performed with HP Chemstation software. The carrier gas flow rate was 1 mL min^{-1}. The oven temperature was kept at 45°C for 4 min and then ramped to 250°C at a rate of 25°C min^{-1}. The injector and detector temperatures were set to 250 and 300°C, respectively.

Experimental Observations and Pseudohomogeneous Reaction Scheme

Reproducibility of experimental results was examined by comparing the rate of hydrogenation at a reference condition (3.5 mol % solution of 1-TMP in 2-methylbutane, 100°C temperature, 1480 kPa pressure, and 500 rpm stirring speed) with different batches of catalyst. These replicates showed that the maximum variation in the rates was about ±2%. This variation was assumed to arise from inhomogeneities in the catalyst and a small variation in the initial concentration of the reactants.

Experiments were performed with used catalyst, without exposing to air, to check for any catalyst deactivation during the reaction. After 60 min of reaction at the reference condition where about 80% of the 1-TMP was hydrogenated, the contents of the reactor were vented off and fresh reactants were loaded into the reactor using a sampling bomb and the reaction was continued at the reference condition for another 60 min. The variation in the reaction rate was ±2%, suggesting no significant catalyst deactivation under the reaction conditions studied.

The reaction system for liquid-phase hydrogenation of isooctenes constitutes three phases and requires the consideration of mass transfer in the gas, liquid, and solid phases and through their interfaces. To ensure that the resistances for the gas–liquid and the liquid–solid interface transports have no influence on the hydrogenation kinetics, a direct test was made by running several experiments at different stirring speeds while keeping all other variables constant. The effect of stirring speed on the initial rate of reaction of 1-TMP was studied over the range of 300–700 rpm. It was found that a change in the stirring speed from 300 to 500 rpm has a pronounced effect on the observed initial rate of reaction, given that the rate of reaction at 500 rpm (1.17 mol min^{-1} g cat^{-1}) was significantly higher than the corresponding rate at 300 rpm (1.01 mol min^{-1} g cat^{-1}). This is probably attributable to a higher mass transfer resistance across the gas–liquid and liquid–solid interface at lower stirring speed. However, at a stirring speed of ≥500 rpm, the observed reaction rate was no longer sensitive to the speed of stirring. Thus in all future experiments, the stirring speed was maintained at 500 rpm. The use of a well-stirred condition implies that the convective mixing of bulk liquid phase is quite vigorous and no significant concentration gradient exists in the bulk liquid phase and at the liquid–solid interface.

The experimental procedure followed in the liquid-phase hydrogenation of isooctenes resembles a situation like that of a slurry reactor where the solid catalyst particles are dispersed in an agitated liquid phase. Thus, the mass transfer treatment for slurry reactor as suggested by Satterfield[16] is followed. Assuming an irreversible pseudo-first-order reaction system (that is, the reaction is first order with respect to hydrogen), and that it occurs entirely on the external surface of the porous catalyst particle, the corresponding rate equation can be expressed as

$$\frac{1}{r_{initial}} = \left(\frac{1}{k_{GL}a_{GL}}\right)\frac{1}{c_{H_2}} + \frac{\rho_S d_P}{6c_{H_2}}\left[\frac{1}{k_{LS}} + \frac{1}{k}\right]\frac{1}{m_{catalyst}} \qquad (1)$$

For a series of experiments where only the catalyst loading was varied, the plot of $(1/r_{initial})$ should be linear with respect to $(1/m_{catalyst})$ with an intercept = $(1/k_{GL}a_{GL})(1/c_{H_2})$. When the catalyst loading is large [that is, $(1/m_{catalyst}) \rightarrow 0$], the rate becomes controlled by the rate of transfer of hydrogen from the gas phase to the liquid phase. Thus, the above intercept represents the rate of the reaction that would be obtained if the reaction is controlled by the gas–liquid mass transfer resistances. To be certain that the gas–liquid mass transfer is not controlling, the actual experimental value of $(1/r_{initial})$ should be much larger than the intercept.

Figure 2 shows the reciprocal of initial rate of the reaction of 1-TMP as a function of the reciprocal of the catalyst mass. Extrapolating the catalyst mass to an infinitely high value (intercept of *y*-axis) gives an estimate of the external gas–liquid mass transfer rate. The obtained intercept was 0.1931 min g cat

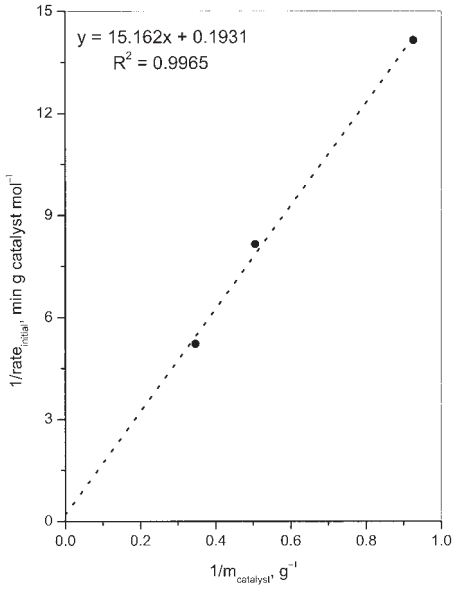

Figure 2. Effect of gas–liquid mass transport on the kinetics of liquid-phase hydrogenation of isooctenes in semi-batch reactor.

Plot of $(1/r_{initial})$ vs. $(1/m_{catalyst})$ according to Eq. 1. Initial reactant: 3.6 mol % 1-TMP, reaction temperature: 100°C; system pressure: 1480 kPa (200 psig); stirring speed: 500 rpm.

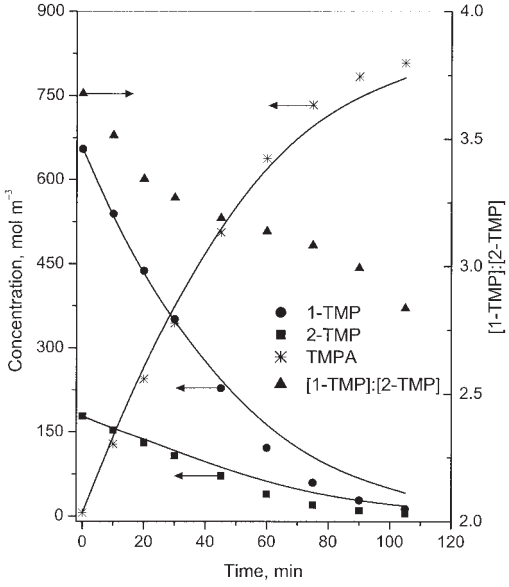

Figure 3. Typical concentration–time profile for the liquid-phase hydrogenation of isooctenes in a semi-batch reactor.

Initial reactant: a mixture of 1-TMP and 2-TMP in a ratio of 3.7:1; reaction temperature: 100°C; system pressure: 1480 kPa (200 psig); stirring speed: 500 rpm; amount of catalyst: 1.13 g. The continuous lines are predictions from the dynamic model.

mol^{-1}. The experimentally observed values of $(1/r_{initial})$ were higher than the above intercept by more than an order of magnitude, suggesting that the gas–liquid mass transfer did not have an effect on the hydrogenation kinetics in the current study. However, from a design perspective, the intraparticle diffusional resistances cannot be ignored, and knowledge of the intrinsic kinetic rate expression free from any mass transport inhibition is required.

Results of kinetic experiments showed palladium to be a very active catalyst for the hydrogenation of isooctenes. A typical profile of concentration vs. the reaction time is shown in Figure 3, which indicates that after 60 min of reaction the conversion of 1-TMP and 2-TMP are 81.5 and 78.3%, respectively, when starting with a mixture of 1-TMP and 2-TMP in a molar ratio of 3.7:1, at a reaction temperature of 100°C, a system pressure of 1480 kPa, and a stirring speed of 500 rpm. Besides isooctane, no other saturated products were formed. It is known that the equilibrium between 1-TMP and 2-TMP is slow.[15] The ratio of the concentration of 1-TMP to 2-TMP is also shown in Figure 3, which decreased as a function of time, apparently indicating that 2-TMP is hydrogenated slower than 1-TMP. However, a significantly different result was obtained when the reaction was carried out with either one of the two pure isomers. Figure 4 shows the time–composition profile when the initial reactant was 1-TMP and Figure 5 shows a similar profile when the initial reactant was 2-TMP. In both cases the double-bond isomerization was significant, although the hydrogenation rates of both isomers exceeded the double-bond isomerization rate because the amount of hydrogenated product (that is, isooctane) always exceeded the amount of isomerization product.

The qualitative dependency of the system pressure on the relative extent of hydrogenation and isomerization can be seen in Figures 6 and 7 for 1-TMP and 2-TMP, respectively. It was observed that the hydrogenation rates increased by a greater degree than the isomerization rate. Therefore, the relative importance of the double-bond isomerization decreased with in-

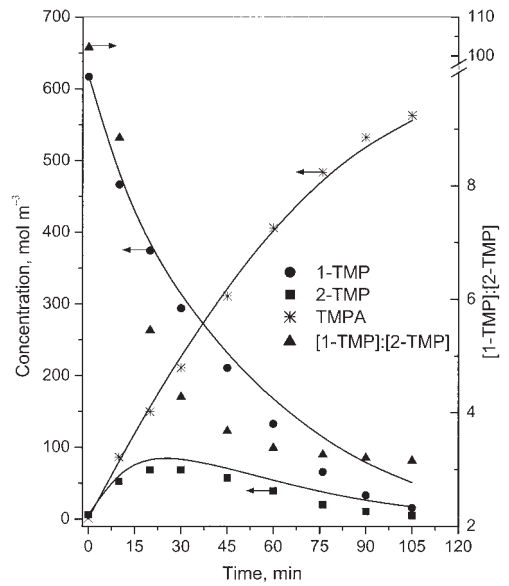

Figure 4. Concentration–time profile for the liquid-phase hydrogenation of isooctenes in a semi-batch reactor.

Initial reactant: 1-TMP; reaction temperature: 110°C; system pressure: 1380 kPa (175 psig); stirring speed: 500 rpm; amount of catalyst: 1.07 g. The continuous lines are predictions from the dynamic model.

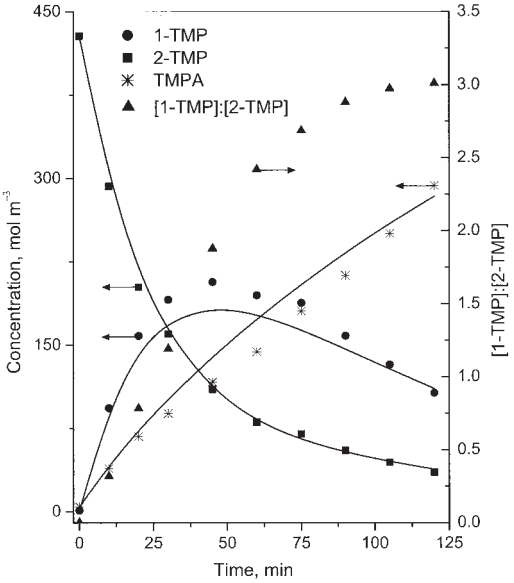

Figure 5. Concentration–time profile for the liquid-phase hydrogenation of isooctenes in a semi-batch reactor.

Initial reactant: 2-TMP; reaction temperature: 110°C; system pressure: 963 kPa (125 psig); stirring speed: 500 rpm; amount of catalyst: 1.09 g. The continuous lines are predictions from the dynamic model.

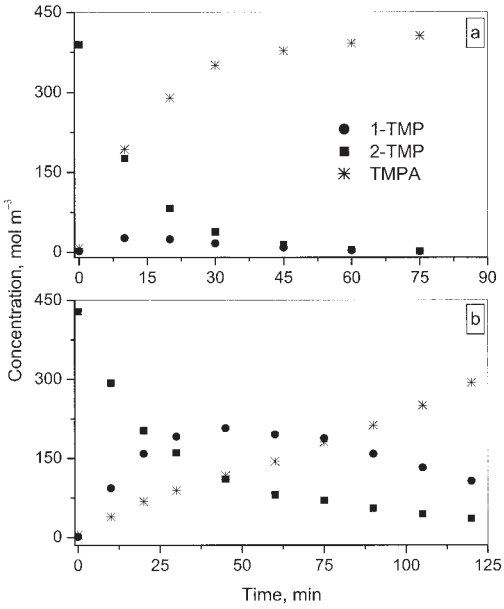

Figure 7. Effect of system pressure on the kinetics of liquid-phase hydrogenation of isooctenes in a semi-batch reactor.

Initial reactant: 2-TMP; reaction temperature: 110°C; stirring speed: 500 rpm; system pressure: (a) 2860 kPa (400 psig), (b) 963 kPa (125 psig); amount of catalyst: (a) 1.09 g, (b) 1.09 g.

creasing hydrogen pressure and also the extent of olefin conversion. The above point was further clarified when the ratio of 1-TMP/2-TMP was plotted against reaction time for two different reactions starting with either of the pure isomers, as shown in Figures 6 and 7. The corresponding plot is shown in Figure 8. It is evident from Figure 8 that starting the reaction with either 9.1 mol % 1-TMP or 6.1 mol % 2-TMP, the molar

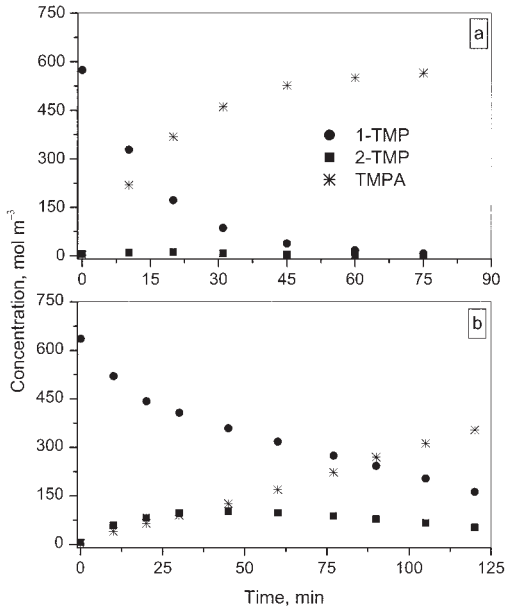

Figure 6. Effect of system pressure on the kinetics of liquid-phase hydrogenation of isooctenes in a semi-batch reactor.

Initial reactant: 1-TMP; reaction temperature: 110°C; stirring speed: 500 rpm; system pressure: (a) 2860 kPa (400 psig), (b) 963 kPa (125 psig); amount of catalyst: (a) 1.15 g, (b) 1.16 g.

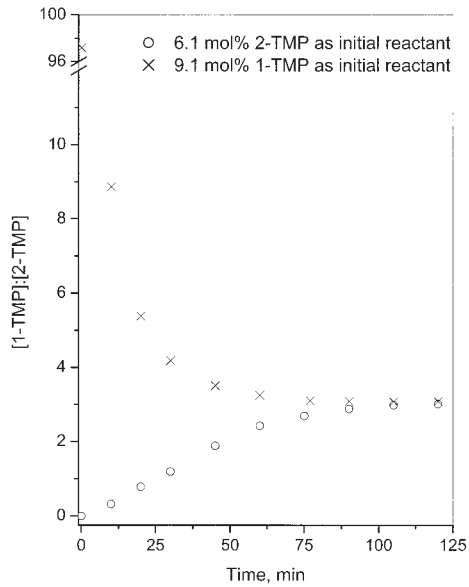

Figure 8. Molar ratio of 1-TMP to 2-TMP plotted against reaction time for two different reactions shown in Figures 6 and 7 in the liquid-phase hydrogenation of isooctenes in a semi-batch reactor.

Initial reactant: 6.1 mol % 1-TMP or 9.1 mol % 2-TMP; system pressure: 963 kPa; reaction temperature: 110°C; stirring speed: 500 rpm.

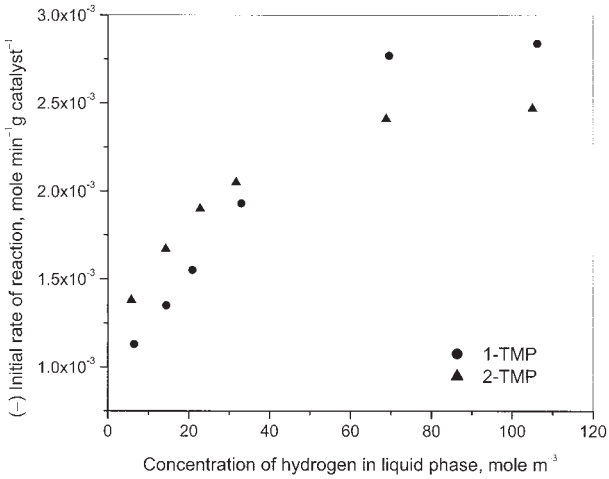

Figure 9. Effect of concentration of hydrogen in the liquid phase on the initial rate of hydrogenation of 1-TMP and 2-TMP.

Reaction temperature: 110°C; stirring speed: 500 rpm; concentration of 1-TMP: 9 mol %; concentration of 2-TMP: 6 mol %.

ratio of 1-TMP/2-TMP reached the equilibrium value of about 3 after 90 min of reaction when the average conversion was about 85%. This also suggests a slower isomerization compared to hydrogenation. The extent of isomerization was higher when the starting reagent was 2-TMP rather than 1-TMP because the latter has greater thermodynamic stability than the former.[15] Thus both the rate of hydrogenation and rate of isomerization were found to be higher for 2-TMP than for 1-TMP over the concentration range studied.

The influence of hydrogen concentration in the liquid phase on the rate of reaction was investigated by adopting a pseudohomogeneous reaction scheme where the rate of reaction was expressed using a power-law kinetic model. The effect of liquid-phase hydrogen concentration on the initial rate of reaction of 1-TMP and 2-TMP is shown in Figure 9, which shows that the initial rates were influenced to a greater extent when the concentration of hydrogen in the liquid phase was <50 mol m^{-3} or when the partial pressure of hydrogen in the system was <800 kPa. However, at a concentration of ≥ 65 mol m^{-3}, the initial rate of reaction becomes less sensitive to the hydrogen concentration. This observed hydrogenation rate, however, is a global rate and does not necessarily follow the true (that is, intrinsic) dependency on the hydrogen concentration. The rate of TMPA formation is governed by the internal diffusion of hydrogen and TMPA; thus, increasing the concentration of the reactants would not proportionately increase the hydrogenation rate. Another possibility may be explained by the fact that at higher hydrogen concentration the surface of the catalyst becomes saturated with adsorbed hydrogen species and the isooctenes act as the limiting reagent. Similar trends, also reported in the literature,[17] indicate the competitive adsorption of hydrogen and isooctenes on a similar type of active site on the catalyst surface. The apparent order of reaction with respect to hydrogen concentration was computed by fitting the initial rate of reaction and concentration of hydrogen in the liquid phase into a power-law rate equation. The resulting order of reaction were found to be between 0.06 and 0.44, depending on hydrogen concentration, which could suggest dissociative adsorption of hydrogen on the active sites.[18]

It should be noted that the concentration of hydrogen on the catalyst surface is different from the concentration of hydrogen in the bulk liquid phase as shown in Figure 9 and there is a concentration gradient inside the catalyst particle. Thus a pseudohomogeneous model will not depict the kinetics correctly and that internal diffusion phenomena should be accounted for. Therefore we developed an intrinsic kinetic model where intraparticle diffusion effects were taken into account and the model is presented in the following sections.

Effects of reaction temperature on the extent of hydrogenation and isomerization are shown in Figure 10 and 11 for 1-TMP and 2-TMP, respectively. It is evident from these figures that the isomerization of 1-TMP to 2-TMP is less dependent on temperature than the isomerization of 2-TMP to 1-TMP, suggesting a lower activation energy for isomerization of 1-TMP to 2-TMP. The rate of hydrogenation of both isomers did not exhibit a big difference by changing the temperature from 70 to 130°C, which suggested that the hydrogenation reaction may be diffusion limited. Figure 12 represents the Arrhenius-type of plot using 2-TMP as the initial reactant over the temperature range studied. The value of activation energy estimated from this plot was found to be in the range of 14–15 kJ mol^{-1}. The low magnitude of activation energy suggests that pore diffusion effects on the kinetics were not eliminated and intraparticle diffusion effects need to be considered for the development of an intrinsic kinetic model.

There are two ways of interpreting the above results. Lylykangas et al.[6] adopted the view that the extent of isomerization was insignificant and could therefore be neglected. The other way to explain the above observations would be to take into

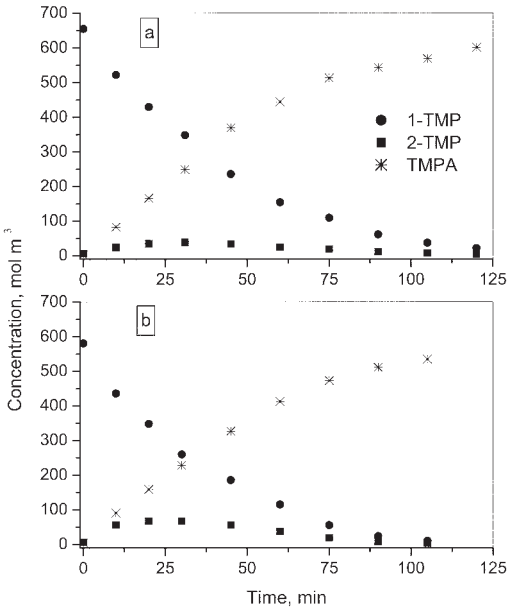

Figure 10. Effect of reaction temperature on the kinetics of liquid-phase hydrogenation of isooctenes in a semi-batch reactor.

Initial reactant: 1-TMP; reaction temperature: (a) 130°C, (b) 70°C; stirring speed: 500 rpm; system pressure: 1480 kPa (200 psig); amount of catalyst: (a) 1.09 g, (b) 1.04 g.

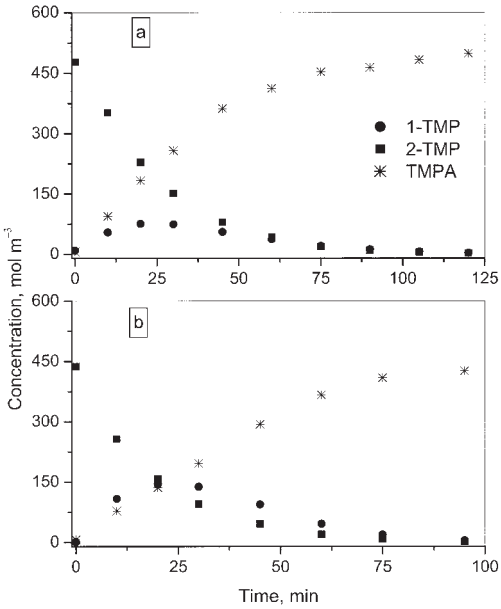

Figure 11. Effect of reaction temperature on the kinetics of liquid-phase hydrogenation of isooctenes in a semi-batch reactor.

Initial reactant: 2-TMP; reaction temperature: (a) 130°C, (b) 70°C; stirring speed: 500 rpm; system pressure: 1480 kPa (200 psig); amount of catalyst: (a) 1.09 g, (b) 1.05 g.

account the isomerization. Indeed our experimental data showed that isomerization is significant whether the initial reactant was 1-TMP or 2-TMP. In the case of using a mixture of 1-TMP and 2-TMP with high concentration of 1-TMP as the reactant, and because the rate of hydrogenation of 1-TMP was lower than that of 2-TMP, a substantial amount of 1-TMP was

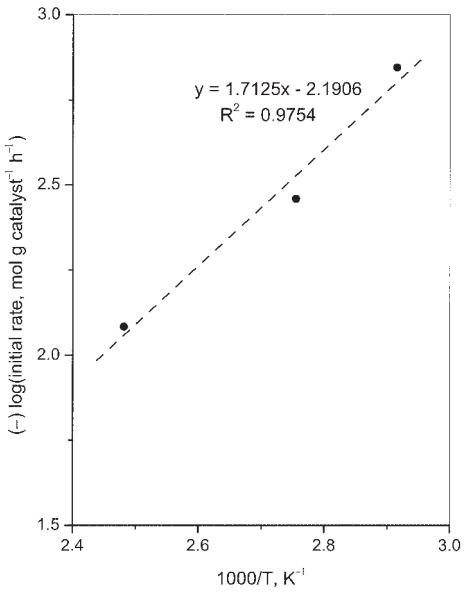

Figure 12. Effect of temperature on the initial rate of hydrogenation of isooctenes.

Arrhenius-type of plot using 2-TMP as the initial reactant in the temperature range studied. Initial reactant: 2-TMP; system pressure: 1480 kPa (200 psig); stirring speed: 500 rpm.

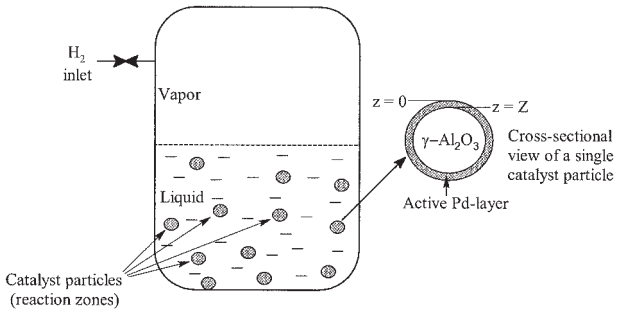

Figure 13. Semi-batch reaction system considered for the model development.

isomerized to 2-TMP, which was hydrogenated at a faster rate, thus apparently showing no reverse isomerization. Because a large amount of 2-TMP was formed from the isomerization of 1-TMP, the apparent rate of disappearance of 2-TMP appears to be much lower than that of 1-TMP. These observations have been substantiated when experiments were done using either of the pure isomers.

Reactor Model for Hydrogenation in Semibatch Mode

Each experiment was modeled as a three-phase, unsteady-state process. The entire reactor volume can be divided into two parts: the vapor phase and the liquid phase containing dispersed solid catalysts. The vapor and liquid phases were well mixed as a result of very efficient stirring. Thus, the vapor and liquid phases were assumed to be in equilibrium with each other at all times. The solid catalyst had an eggshell-type of distribution of palladium on its surface. The thickness of the palladium layers on the inert support was very small (that is, an average thickness of 0.5 mm) and was only 8% of the dimension of the catalyst. The region of the catalyst where the reaction takes place can therefore be assumed to have a rectangular geometry. The reactor was maintained at a constant temperature and the hydrogen pressure was held constant by supplying hydrogen continuously as it was consumed by the reaction; thus the reactor system can be considered as a semi-batch mode. The reaction system used in the model development is shown in Figure 13.

The dynamic reactor model consists of the material balance of each component in the vapor and liquid phases. Because the vapor and liquid phases are in equilibrium, the mass transfer rate between these two phases was infinitely large and a material balance of the sum of each component in the two phases can be written as:

$$\frac{d}{dt}\left(n_i^L + n_i^V\right) = -AN_i\big|_{z=0} \qquad i = 1, \ldots, 5 \tag{2}$$

Component i varies from 1 to 5 corresponding to 1-TMP, 2-TMP, TMPA, isopentane, and n-heptane, respectively. For hydrogen, the above material balance cannot be written because hydrogen was continuously fed into the reactor to maintain constant pressure. The material balance for hydrogen can be replaced by the following equation:

$$V^R = \frac{\sum n_i^L}{\rho^L} + \frac{\sum n_i^V}{\rho^V} \qquad i = 1, \ldots, 6 \tag{3}$$

The numbers of moles of each component in the vapor and the liquid phases are related through the following equilibrium relationship:

$$K_i^{eq} \frac{n_i^L}{\sum n_j^L} = \frac{n_i^V}{\sum n_j^V} \qquad i = 1, \ldots, 5; j = 1, \ldots, 6 \tag{4}$$

$$\frac{n_6^V}{\sum n_j^V} P^{total} = H \frac{n_6^L}{\sum n_j^L} \qquad j = 1, \ldots, 6 \tag{5}$$

The reported values of the Henry's law constant for hydrogen in each of the pure components were used.[19] To calculate the Henry's law constant for hydrogen in the liquid mixture, a combination rule was used.[20] The vapor–liquid equilibrium constant values were calculated from Smith and Van Ness.[21] The activity coefficients were computed from the modified UNIQUAC method and the vapor fugacity coefficients were calculated by the virial equation.[22]

The above set of equations could be solved only if the value of N_i at $z = 0$ is specified. To obtain the values of N_i, the concentration gradient at $z = 0$ must be known or, in other words, the concentration profile within the catalyst must be known. Determination of the concentration profile would require the solution of the following mass-balance equations within the catalyst particle:

$$\varepsilon_P \frac{\partial c_i}{\partial t} + \frac{\partial N_i}{\partial z} = r_i \rho_S \qquad i = 1, \ldots, 6 \tag{6}$$

$$N_i \cong -D_{eff}^i \frac{\partial c_i}{\partial z} \qquad i = 1, \ldots, 6 \tag{7}$$

The values of the effective diffusivities were obtained from the following relation:

$$D_{eff}^i = \frac{\varepsilon_P}{\tau_P} D_m^i \qquad i = 1, \ldots, 6 \tag{8}$$

Molecular diffusion coefficients of the mixture (D_m^i) were calculated from the binary diffusion coefficients and liquid-phase molar fractions. The binary diffusivities and the diffusivity in the mixture were estimated by the Wilke–Chang method.[20] The porosity and tortuosity values of the catalyst particles were approximated to the corresponding average values for aluminum oxide (that is, 0.5 and 4.0, respectively).[16] Substituting Eq. 7 into Eq. 6, and considering that D_{eff}^i is independent of z, results in the following equation:

$$\varepsilon_P \frac{\partial c_i}{\partial t} - D_{eff}^i \frac{\partial^2 c_i}{\partial z^2} = r_i \rho_S \qquad i = 1, \ldots, 6 \tag{9}$$

The reaction rate terms must be supplied before the above system of equations can be solved. Because the experiments were performed under isothermal conditions, the energy balances for the bulk phases were not needed. Furthermore, calculations showed that, under the experimental conditions applied, the maximum temperature difference inside the catalyst particle was <0.2°C. Thus the energy balance for the particle was also omitted.

Intrinsic Kinetic Model for Heterogeneous Hydrogenation

The mechanism generally accepted for noble-metal–catalyzed olefin hydrogenation is the Horiuti–Polanyi reaction sequence.[23] According to the classic Horiuti–Polanyi mechanism, the olefin is chemisorbed in a di-σ-adsorbed form on the catalyst surface, accompanied by the cleavage of the double bond and a two-step addition of dissociatively adsorbed hydrogen. The addition of hydrogen to the "half-hydrogenated" intermediate is essentially irreversible under common experimental hydrogenation conditions but the other steps are all potentially reversible. This reversibility also accounts for the double-bond isomerization that frequently occurs during hydrogenation of olefins.

However, recent spectroscopic and theoretical studies have shown that it is probably the π-adsorbed form of the olefins, which appears as the primary adsorption species during the hydrogenation on Pd/γ-Al_2O_3 catalysts.[14,24-26] Although the original Horiuti–Polanyi mechanism assumes that the olefin intermediate is di-σ-adsorbed, it still does capture the main features of the hydrogenation reaction, and is still likely to be valid even if a surface π-adsorbed olefin intermediate is involved. Thus in the current study, a "Horiuti–Polanyi type" of mechanism involving a surface π-adsorbed species on a single active site was adopted. The reason for not considering the π-allyl–type of intermediate will be discussed later in the Results and Discussion section. The dissociative chemisorption of hydrogen on palladium has been reported by several researchers.[12,27] On the basis of the above observations and results from the kinetic experiments, the following intrinsic kinetic model was proposed for the hydrogenation of isooctenes on the Pd/γ-Al_2O_3 catalyst.

Model assumptions and development

The following assumptions are made to develop the intrinsic kinetic model: molecular adsorption of isooctenes (in surface π-adsorbed mode) and dissociative adsorption of hydrogen on the same type of active sites, equilibrium concentration of adsorbed species, surface reaction between adsorbed isooctene, and hydrogen species as the rate determining step (RDS). The reaction steps and corresponding rates are shown in Table 2.

Dehydrogenation of isooctane on palladium was ignored (that is, $k_e = 0$) because the adsorption of saturated hydrocarbons is weaker than the adsorption of the corresponding olefins, and the dehydrogenation will occur only at considerably higher temperature and would not be thermodynamically feasible under the present operating conditions.[28] Isomerization between 1-TMP and 2-TMP was assumed to take place by the common half-hydrogenated intermediate, C^*. Experimental evidence for this was obtained by performing experiments at the same temperature and pressure with a mixture of 1-TMP and 2-TMP, but in the absence of hydrogen (in a nitrogen atmosphere). In such cases, no traces of isomerization products were

Table 2. Proposed Reaction Sequence and Rate Expressions in the Liquid-Phase Hydrogenation of Isooctenes*

Step	Reaction	Rate
1	$A + S \underset{k_{-A}}{\overset{k_A}{\rightleftharpoons}} AS$	$k_A C_A \theta_S - k_{-A}\theta_{AS}$
2	$B + S \underset{k_{-B}}{\overset{k_B}{\rightleftharpoons}} BS$	$k_B C_B \theta_S - k_{-B}\theta_{BS}$
3	$H_2 + 2S \underset{k_{-H_2}}{\overset{k_{H_2}}{\rightleftharpoons}} 2HS$	$k_{H_2} c_{H_2} \theta_S^2 - k_{-H_2}\theta_{HS}^2$
4	$AS + HS \underset{k_{b1}}{\overset{k_{f1}}{\rightleftharpoons}} C^*S + S$	*RDS*
5	$BS + HS \underset{k_{b2}}{\overset{k_{f2}}{\rightleftharpoons}} C^*S + S$	*RDS*
6	$C^*S + HS \underset{k_e}{\overset{k_d}{\rightleftharpoons}} DS + S$	$k_d \theta_{C^*S}\theta_{HS} - k_e \theta_{DS}\theta_S$
7	$DS \underset{Fast}{\overset{k_f}{\longrightarrow}} D + S$	$k_f \theta_{DS}$

*A, 1-TMP; B, 2-TMP; D, TMPA; S, active site on catalyst surface; C^*, half-hydrogenated intermediate.

obtained. This also confirmed that the hydrogenation of isooctene proceeds by a mechanism involving surface π-adsorbed species and not by π-allyl intermediate, given that isomerization by π-allyl intermediate can proceed without the presence of hydrogen.[12] Also a slow isomerization rate compared with the hydrogenation rates in the kinetic experiments implied rate limitation for the first hydrogen addition to the double bonds of adsorbed 1-TMP and 2-TMP. Because the formation of the common intermediate C^* from a mixture of 1-TMP and 2-TMP takes place by two completely different reactions, it is necessary to consider two different RDS in the development of the kinetic model.

In the reaction mechanism considered, steps 1, 2, and 3 are assumed to be fast enough for the quasi-equilibrium hypothesis to be applied. The terms K_A, K_B, and K_{H_2} denote the corresponding adsorption equilibrium constants. Thus the following equations can be written:

$$\theta_{AS} = K_A c_A \theta_S \tag{10}$$

$$\theta_{BS} = K_B c_B \theta_S \tag{11}$$

$$\theta_{HS} = \sqrt{K_{H_2} c_{H_2}}\,\theta_S \tag{12}$$

Step 7 was assumed to be rapid and irreversible, which implies that $\theta_{DS} = 0$. The pseudo-steady-state assumption was applied for the half-hydrogenated intermediate C^*:

$$k_{f1}\theta_{AS}\theta_{HS} + k_{f2}\theta_{BS}\theta_{HS} = k_d \theta_{C^*S}\theta_{HS} + (k_{b1} + k_{b2})\theta_{C^*S}\theta_S \tag{13}$$

A total balance of the active sites of the catalyst results in

$$\theta_S = 1 - \theta_{AS} - \theta_{BS} - \theta_{C^*S} - \theta_{HS} - \theta_{DS} \tag{14}$$

When Eqs. 10–13 were solved along with Eq. 14, the surface coverage could be expressed as a function of bulk concentration as follows:

$$\theta_S = \frac{1}{1 + K_A c_A + K_B c_B + \sqrt{K_{H_2} c_{H_2}} + \alpha} \tag{15}$$

where

$$\alpha = \frac{k_{f1} K_A c_A \sqrt{K_{H_2} c_{H_2}} + k_{f2} K_B c_B \sqrt{K_{H_2} c_{H_2}}}{k_d \sqrt{K_{H_2} c_{H_2}} + k_{b1} + k_{b2}}$$

Thus, the reaction rate for 1-TMP and 2-TMP can be expressed as

$$r_A = -k_{f1}\theta_{AS}\theta_{HS} + k_{b1}\theta_{C^*S}\theta_S = (-k_{f1} K_A \sqrt{K_{H_2} c_{H_2}} c_A + k_{b1}\alpha)\theta_S^2 \tag{16}$$

$$r_B = -k_{f2}\theta_{BS}\theta_{HS} + k_{b2}\theta_{C^*S}\theta_S = (-k_{f2} K_B \sqrt{K_{H_2} c_{H_2}} c_B + k_{b2}\alpha)\theta_S^2 \tag{17}$$

However, using the solutions of Eqs. 16 and 17 will require a large number of constants to be evaluated. Thus some simplifying assumptions were made to change the kinetic model into a form involving fewer constants. Because the reactor was maintained at constant hydrogen pressure, c_{H_2} did not vary much during an experiment and the term in the denominator of α can be considered roughly constant. Furthermore, because the reactant to catalyst ratio was very high, θ_S was considered as constant. Making these simplifying assumptions, the following simplified rate equations for hydrogenation of 1-TMP and 2-TMP were obtained after replacing the parameter groups by lumped parameters, k_{F1}, k_{F2}, k_{B1}, and k_{B2}:

$$r_A = (-k_{F1} c_A + k_{B1} c_B)\sqrt{c_{H_2}} \tag{18}$$

$$r_B = (-k_{F2} c_B + k_{B2} c_A)\sqrt{c_{H_2}} \tag{19}$$

The rate of formation of TMPA can be expressed as

$$r_D = -r_A - r_B \tag{20}$$

The above equations involve the evaluation of only four rate constants. The validity of the above assumptions can be justified from the fit of the experimental results to the above rate equations.

Solution of Model Equations and Parameter Estimation

The mass balance of each component in the liquid phase was coupled with the mass-balance equation in the catalyst phase through the term N_i at $z = 0$. There are two ways of solving the above coupled system of equations. One way would be to solve

the ordinary differential equation (ODE) for the liquid phase independently of the partial differential equation (PDE) in the solid phase. In this case the time steps should be such that the N_i at $z = 0$ should be constant during each time step. The other approach will be to solve the coupled ODE–PDE set simultaneously, which was adopted in the current study.

The finite-difference method has been used in the discretization of the catalyst mass-balance equations. A fully implicit scheme has been adopted. Because the intensity of reaction was very strong near the catalyst surface compared to that inside the catalyst particle, a closely spaced grid network was required near the surface. A typical simulation problem can be solved by dividing the entire reaction zone into several hundreds of equally spaced grid points. It should be noted that such an approach is impractical for the optimization problem, given that during an optimization procedure each simulation needs to be performed several hundred times. On the other hand, use of uniform grid spacing with the above number of grid points will yield a false impression of rate constants, which will be much larger. Additionally, there will be a waste of computation effort because most of the grid points will span regions of the catalyst where the concentration profile would be flat. Therefore it is very crucial to reduce the number of grid points to speed up the procedure. A few initial simulations showed that the concentration profiles vary steeply within a very short distance from the catalyst surface. Therefore a very fine mesh was adopted in this short region and a coarse grid was adopted in the interior of the catalyst particle. Thus some 20–30 grid points were sufficient to capture the system dynamics accurately. The discretized equations along with a representative grid segment are shown in the Appendix.

The concentration of the reactants on the catalyst surface (on the first node) was considered to be the same as that of the bulk fluid. The concentration gradient at the innermost node was assumed zero. Therefore, the c_i values for the first node can be written in terms of the n_i^L. A system of nonlinear algebraic equations involving $[2n + (m - 2)n]$ variables and equations were obtained.

The initial condition for the above system of equations involved specifying the total weight of the reactants initially charged into the reactor, the concentration of each component in the liquid phase, the temperature, and the total pressure. Because the system of equations was nonlinear, the value of the variables at the end of each time step was determined by Newton's method. In each Newton's iteration, the values of the constants at the $(j + 1)$th time was assumed the same as that at the jth time. This assumption can be made because the change in properties of the fluid was small during each time step. Moreover the values of these constants were recalculated at the end of each time step. The resulting Jacobian has a typical block tridiagonal structure with inner submatrices. A sparse matrix solver in Matlab 6.5® was thus used to determine the updated values.

Parameter estimation was performed simultaneously with the solution of the above system of nonlinear algebraic equations. The unknown values of the rate constants were estimated through the minimization of the objective function (O.F.). The O.F. to be minimized was the sum of squares of the errors between the experimental and calculated concentration of the liquid products

$$\text{O.F.} = \sum_j \sum_i (c_i^{\text{exp}} - c_i^{\text{cal}})_j^2 \tag{21}$$

where j denotes analyzed product samples and i is the component index. The minimization of Eq. 21 was done with the FMINCON routine in Matlab 6.5®, which is a subspace trust region method and is based on an interior-reflective Newton method.[29,30] All the reaction rate constants were assumed to be a function of temperature according to the following expression:

$$k_i = k_i^{ref} \exp\left[-\frac{E_i^{app}}{R} \left(\frac{1}{T} - \frac{1}{T_{ref}} \right) \right] \tag{22}$$

where 110°C was chosen as the reference temperature, T_{ref}. Thus the estimated parameters were reaction rate constants at the reference temperature and apparent activation energies.

The significance of the overall regression is tested by means of an F-test performed at the 95% probability level.[31] The ratio defined in Eq. 23 was determined while performing this test. The error covariance matrix $\underline{\underline{\sigma_{hk}}}$ was estimated from a single replicate experiment according to Eq. 24.

$$F_c = \frac{\sum_{h=1}^{2} \sum_{k=1}^{2} \underline{\underline{\sigma_{hk}}} \sum_{i=1}^{n} (\hat{r}_{ih} \hat{r}_{ik})/p}{\sum_{h=1}^{2} \sum_{k=1}^{2} \underline{\underline{\sigma_{hk}}} \sum_{i=1}^{n} (r_{ih} - \hat{r}_{ih})(r_{ik} - \hat{r}_{ik})/(2n - p)} \tag{23}$$

$$\underline{\underline{\sigma_{hk}}} = \left[\frac{\sum_{i=1}^{n_e} (r_{ih} - \bar{r}_h)(r_{ik} - \bar{r}_k)}{n_e - 1} \right] \tag{24}$$

The subscripts h and k in Eqs. 23 and 24 indicate responses and may take the value of 1, 2, or 3, depending on whether the responses are the concentration of 1-TMP, 2-TMP, or TMPA, respectively; n is the number of experiments; p is the number of parameter; $\bar{r}_h$ is the mean of the hth response; and $\hat{r}_{ih}$ denotes the simulated value of the ith observation for the hth response. The value of F_c is 1077.4 with 8 and 272 degrees of freedom. Because this ratio is much larger than the tabulated α percentage point (with $\alpha = 0.05$) of the F distribution, the regression was considered meaningful.

Results and Discussion

Experiments were conducted at temperatures ranging from 70 to 130°C and pressures ranging from 125 to 400 psig (963 to 2860 kPa absolute). The composition of the mixtures in the different experiments were varied from a maximum of 9.5 mol % (14 wt %) to 0.01 mol % (0.04 wt %) 1-TMP and a maximum of 6.5 mol % (10 wt %) to 0.08 mol % (0.12 wt %) of 2-TMP. The results of the F-test at the 95% probability level performed using all experimental data points from the above set of experiments showed that the fitting was meaningful. The model parameters estimated along with 95% confidence interval level are presented in Table 3. In addition, values of the

Table 3. Estimated Model Parameters with 95% Confidence Intervals for the Liquid-Phase Hydrogenation of Isooctenes and RSS and RRMS Values of All the Data Points*

Parameter	Estimated Value
$k_{F1,ref}$, $\frac{\text{mol}}{(\text{s})(\text{kg cat})} \times \left(\frac{\text{m}^3}{\text{mol}}\right)^{3/2}$	$(6.3 \times 10^{-4}) \pm 1 \times 10^{-5}$
$k_{F2,ref}$, $\frac{\text{mol}}{(\text{s})(\text{kg cat})} \times \left(\frac{\text{m}^3}{\text{mol}}\right)^{3/2}$	$(17.1 \times 10^{-4}) \pm 6 \times 10^{-5}$
$k_{B1,ref}$, $\frac{\text{mol}}{(\text{s})(\text{kg cat})} \times \left(\frac{\text{m}^3}{\text{mol}}\right)^{3/2}$	$(13.1 \times 10^{-4}) \pm 4 \times 10^{-5}$
$k_{B2,ref}$, $\frac{\text{mol}}{(\text{s})(\text{kg cat})} \times \left(\frac{\text{m}^3}{\text{mol}}\right)^{3/2}$	$(5.1 \times 10^{-4}) \pm 2 \times 10^{-5}$
E_{F1}, J mol^{-1}	$(3.2705 \times 10^4) \pm 12$
E_{F2}, J mol^{-1}	$(3.0084 \times 10^4) \pm 33$
E_{B1}, J mol^{-1}	$(3.9109 \times 10^4) \pm 28$
E_{B2}, J mol^{-1}	$(3.0255 \times 10^4) \pm 38$
RSS, mol m^{-3}	850.93
RRMS, mol m^{-3}	60.32

*The reference temperature for the evaluation of rate constants was chosen as 110°C.

residual sum of squares (RSS) of all the data points and the residual root mean square (RRMS) are presented.

To show the effect of a change of model parameters on TMPA conversion, a test case is considered. In this case, an initial mixture of 620 mol m^{-3} 1-TMP and 169 mol m^{-3} 2-TMP yields a conversion of 92% for TMPA after 105 min at 120°C and 200 psig pressure. Under this situation a 10% increment of k_{F1} causes the value of this conversion to increase to 96%. A similar increment in the value of k_{F2} causes this conversion to increase to 95.3%. Similar increments in the values of k_{B1} and k_{B2} causes the overall conversion to decrease to 88.8 and 88.7%, respectively. Therefore each of these rate coefficients must be accurately determined because a small change in their values causes a significant change in the values of the conversion for TMPA.

The estimated model parameters confirmed the qualitative observations that 2-TMP has higher reactivity than that of 1-TMP. At the reference temperature (110°C) the hydrogenation rate constant for 2-TMP was almost three times the corresponding value for 1-TMP. At the same temperature, the isomerization rate constant for 1-TMP formation (that is, k_{B1}) was almost three times that of the isomerization rate constant for 2-TMP formation (that is, k_{B2}), thus supporting the experimental observations as shown in Figures 4 and 5, that is, the amount of 1-TMP formed is higher when the initial reactant was 2-TMP than the amount of 2-TMP formed when the initial reactant was 1-TMP. The estimated value of isomerization activation energy for 2-TMP formation (that is, E_{B2}) was lower than the corresponding isomerization activation energy of 1-TMP formation (that is, E_{B1}), suggesting a lower temperature dependency of isomerization of 1-TMP compared to 2-TMP (see Table 3). The above trend was also observed in the qualitative analysis of experimental data shown in Figures 10 and 11.

The predictions from the dynamic model for the concentration profile of 1-TMP, 2-TMP, and TMPA are shown in Figures 3, 4, and 5 by the continuous lines. It can be seen that the simulated concentration profiles are in good agreement with the experimental results. The shape of the dynamic model curves closely follows the experimental data points, indicating good agreement with the developed model. Similar experiments carried out at different conditions also showed a good fit of experimental results with the simulated ones. However, analysis of Figure 4 revealed that some slight deviations were observed at low concentration of 1-TMP. Also, it was found that at high pressure (such as 2860 kPa), the model slightly overpredicts the isomerization of 1-TMP and 2-TMP. This can be explained by the fact that the effect of c_{H_2} on k_{B1} and k_{B2} was not considered.

It can be demonstrated that the rate expressions shown in Eqs. 16 and 17 also support the qualitative observation about the dependency of the apparent pseudo-order of reaction on the concentration of hydrogen. At low hydrogen concentration, c_A or $c_B > \sqrt{c_{H_2}}$ and $\alpha \ll 1$; thus $\theta_S \cong 1/c_A$ or $1/c_B$. Therefore the rate of hydrogenation becomes fractional order with respect to hydrogen concentration. This supports the finding of a fractional order dependency on hydrogen concentration using the pseudohomogeneous power-law kinetic model as discussed earlier.

Figures 14 and 15 represent a comparison between the model prediction and experimental concentration of all data points from all experiments for 1-TMP, 2-TMP, and TMPA, respectively. As can be seen from these figures, the model agrees fairly well with the experimental data under all reaction conditions studied. The outliers correspond to the experiments conducted at high pressure.

Findings in the present research that 2-TMP has higher overall reactivity than that of 1-TMP and double-bond isomerization plays a significant role during hydrogenation are in contrast to the results reported by Lylykangas et al.[6–8] using Ni/Al_2O_3, Co/SiO_2, and Pt/Al_2O_3 catalyst. The most likely explanation for observing significant isomerization can be at-

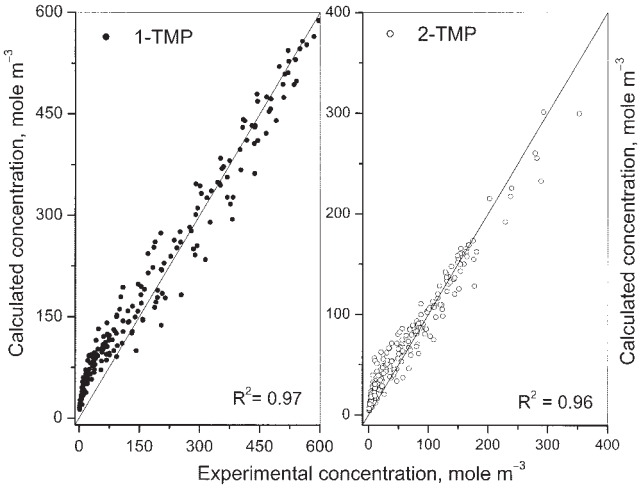

Figure 14. Comparison of the experimental and model predicted concentration of 1-TMP and 2-TMP in the liquid-phase hydrogenation of isooctenes in a semibatch reactor.

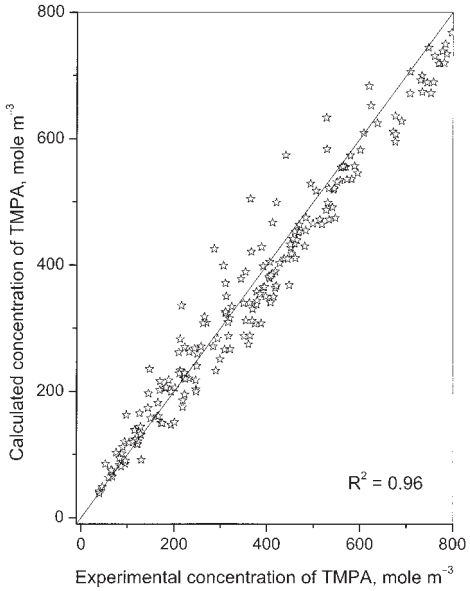

Figure 15. Comparison of the experimental and model-predicted concentration of TMPA in the liquid-phase hydrogenation of isooctenes in a semibatch reactor.

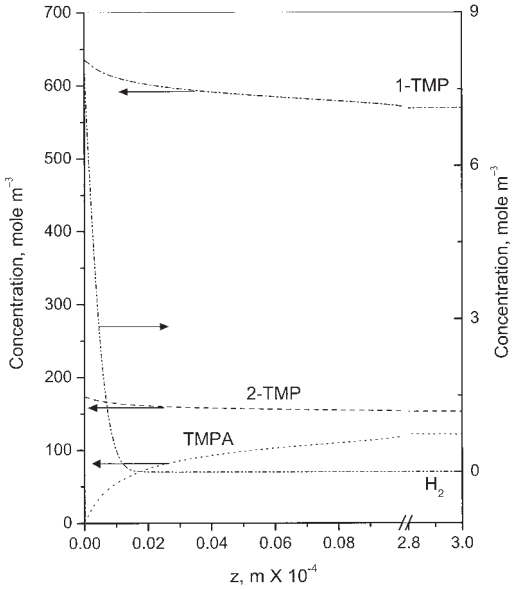

Figure 16. Concentration profile of reactants and products inside catalyst particles after 3600 s of reaction at 110°C and 963 kPa (125 psig) pressure.

The feed was a mixture of 1-TMP and 2-TMP (3.7:1) and the initial concentration of 1-TMP was 9.2 mol %.

tributed to the fact that the extent of double-bond isomerization varies with the nature of the catalyst and decreases in the order: Pd > Ni > Rh > Ru > Os ≈ Ir ≈ Pt.[24,32] It was found in the current research that the order of isomer reactivity can be reversed if double-bond isomerization were neglected. Assuming the extent of isomerization was insignificant as compared to hydrogenation (that is, setting $k_{B1} = k_{B2} = 0$), Eqs. 18 and 19 can be modified as

$$r_A = -k_{F1} c_A \sqrt{c_{H_2}} \tag{25}$$

$$r_B = -k_{F2} c_B \sqrt{c_{H_2}} \tag{26}$$

Following a similar procedure as described earlier, the model parameters of Eqs. 25 and 26 were estimated along with a 95% confidence interval and are shown in Table 4. The estimated model parameters suggest that 1-TMP was more reactive than

Table 4. Estimated Model Parameters of Eqs. 25 and 26 with 95% Confidence Intervals for the Liquid-Phase Hydrogenation of Isooctenes*

Parameter	Estimated Value
$k_{F1,ref}, \frac{\text{mol}}{(\text{s})(\text{kg cat})} \times \left(\frac{\text{m}^3}{\text{mol}}\right)^{3/2}$	$(1.69 \times 10^{-4}) \pm 9 \times 10^{-6}$
$k_{F2,ref}, \frac{\text{mol}}{(\text{s})(\text{kg cat})} \times \left(\frac{\text{m}^3}{\text{mol}}\right)^{3/2}$	$(1.23 \times 10^{-4}) \pm 6 \times 10^{-6}$
E_{F1}, J mol^{-1}	$(1.7449 \times 10^4) \pm 26$
E_{F2}, J mol^{-1}	$(1.0506 \times 10^4) \pm 82$

*The reference temperature for the evaluation of rate constants was chosen as 110°C.

2-TMP, which contradicts the experimental results. This anomaly arises from neglecting the isomerization.

Hydrogenation of both 1-TMP and 2-TMP was severely diffusion limited inside the catalyst particles, even though the thickness of the effective catalyst region (that is, the palladium layer on the support) was only about 0.5 mm. The concentration profile of reactants and products inside the catalyst particle after 3600 s of reaction time is shown in Figure 16. It can be seen that the concentration of isooctenes decreased with time, whereas the concentration of TMPA increased. The concentration of hydrogen was zero within a very thin layer from the surface. Thus hydrogen was the limiting reactant. Although the system pressure was large, the partial pressure of hydrogen was much lower (that is, in an experiment using 5.7 mol % 2-TMP as initial reactant at 110°C and a system pressure of 1480 kPa, the partial pressure of hydrogen was only 640 kPa). Thus, the concentration of hydrogen in the liquid phase was quite low. As a result the concentration of hydrogen on the catalyst surface was low and hydrogen acts as the limiting reagent. Because the hydrogen concentration rapidly drops to zero as a result of consumption by the reaction, most of the catalyst zone thickness remains unused. Thus it would be better to have a very thin eggshell-type distribution of the palladium layer on the support.

However, a completely different scenario was found when the reaction was carried out at a system pressure > 2170 kPa. The concentration profile of reactants and isooctane within the catalyst particle after 3600 s of reaction at 110°C temperature and a system pressure of 2860 kPa is shown in Figure 17. A comparison of Figure 17 with Figure 16 revealed that the concentration of hydrogen on the catalyst surface at 2860 kPa pressure was almost 15 times higher than the corresponding value at 963 kPa. High system pressure also helped to maintain

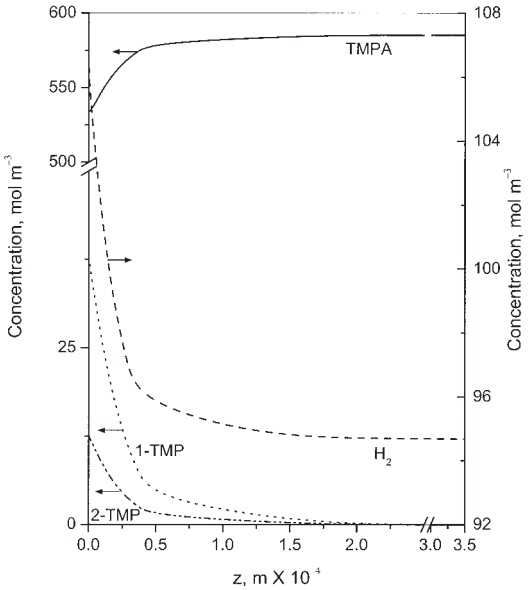

Figure 17. Concentration profile of reactants and products inside catalyst particles after 3600 s of reaction at 110°C and 2860 kPa (400 psig) pressure.

The feed was a mixture of 1-TMP and 2-TMP (3.7:1) and the initial concentration of 1-TMP was 9.2 mol %.

a higher concentration of hydrogen within the catalyst particle. The concentration of isooctenes was found to be almost zero within a very thin layer from the surface and the isooctenes become the limiting reactant. The high concentration of hydrogen makes the rate of reaction almost independent of any further increase in hydrogen concentration. This also explains the experimental result presented in Figure 9, where the magnitude of initial rate of reaction does not show any significant increase by increasing the liquid-phase hydrogen concentration > 65 mol m^{-3}. The above findings also explain the very fast rate of hydrogenation and the slow rate of isomerization at higher system pressure as observed experimentally.

Conclusions

Liquid-phase hydrogenation of isooctenes on a Pd/γ-Al_2O_3 catalyst was studied in a batch reactor operated in semibatch mode at 70–130°C and under constant total pressure at 963–2860 kPa. No catalyst deactivation was observed during the study. In addition to hydrogenation, double-bond isomerization between 1-TMP and 2-TMP was observed. The extent of double-bond isomerization was found to be significant during hydrogenation. However, no isomerization was observed in the absence of hydrogen. The magnitudes of the reactivity of the two isomers were comparable, although 2-TMP was slightly more reactive than 1-TMP toward hydrogenation. The extent of isomerization using pure 2-TMP as reactant was higher than that of 1-TMP.

A kinetic model was developed on the basis of a Horiuti–Polanyi type of mechanism, assuming the formation of the half-hydrogenated intermediate was rate limiting. The dynamic reactor model and the material balance for catalyst particle was solved simultaneously along with the kinetic model. The kinetic parameters were estimated from experimental results by nonlinear regression. Comparison of the experimental and calculated concentrations of all data points showed good agreement with experimental results, and the model can accurately predict the kinetic behavior of the system. It was also shown that at a system pressure < 1480 kPa, the concentration of hydrogen rapidly dropped to zero inside the catalyst particle and hydrogen becomes the limiting reagent. Thus, a very thin eggshell-type distribution of palladium on the support would be more economical. However, at a system pressure > 2170 kPa, the hydrogen concentration inside the catalyst remained very high and the concentration of 1-TMP and 2-TMP decreased to zero within a very thin layer from the catalyst surface. Under such a condition the rate of hydrogenation becomes almost independent of hydrogen concentration and isooctenes constitute the limiting reagent.

Acknowledgments

Financial support from the National Sciences and Engineering Research Council of Canada, Strategic Projects Program, is gratefully acknowledged.

Notation

a_{GL} = effective gas–liquid interfacial area, m^2 m^{-3}
A = total external surface area of the catalyst, m^2
c_i = concentration of component i, mol m^{-3}
C^* = reaction intermediate
d_P = effective diameter of catalyst particle, m
D^i_{eff} = effective diffusivity of component i, m^2 s^{-1}
D^i_m = molecular diffusivity of component i in the mixture, m^2 s^{-1}
E_i^{app} = apparent activation energy corresponding to lumped rate parameter k_i as defined in Eqs. 18 and 19, J mol^{-1}
k_i = rate constant for reaction i at temperature T, K
k_i^{ref}, $k_{i,ref}$ = rate constant for reaction i at reference temperature T_{ref}, K
k_{GL} = gas–liquid mass transfer coefficient, m s^{-1}
k_{LS} = liquid–solid mass transfer coefficient, m s^{-1}
K_i = adsorption equilibrium constant of component i
K_i^{eq} = vapor–liquid equilibrium constant of component i
H = Henry's law constant for hydrogen
$m_{catalyst}$ = mass of catalyst, g or kg
n_e = number of replicate experiments
n_i^L = total number of moles of component i in the liquid phase
n_i^V = total number of moles of component i in the vapor phase
N_i = molar flux of component i in the solid phase, mol m^{-2} s^{-1}
P^{total} = total pressure of the system, kPa
r_i = rate of generation of component i, mol s^{-1} kg cat^{-1}
$\hat{r}_{ih}$ = model value of the hth response in the ith observation
$r_{initial}$ = initial rate of generation of component i, mol s^{-1} kg cat^{-1}
R = universal gas constant [$\equiv$8.314 J mol^{-1} K^{-1}]
T = temperature, °C or K
T_{ref} = reference temperature [$\equiv$383.15 K]
t = time variable, s, min, or h
V^R = volume of the reactor, m^3
z = distance, m

Greek letters

ε_P = porosity of the catalyst particle
ρ^L = density of the liquid phase, mol m^{-3}
ρ^V = density of the vapor phase, mol m^{-3}
ρ_S = bulk density of the catalyst, kg m^{-3}
θ_i = fraction of the active sites of catalyst surface covered by component i
τ_P = tortuosity of the catalyst particle

Subscripts and superscripts

A = 1-TMP
B = 2-TMP

cal = calculated
eq = equilibrium
exp = experimental
i, j, k = component index, discretization point index
l = reaction index to rate parameters as defined in Eqs. 18 and 19
G = gas phase
GL = gas–liquid interface
H_2 = hydrogen
L = liquid phase
LS = liquid–solid interface
n = number of components
P = catalyst particle
R = reactor
ref = reference temperature (383.15 K)
S = solid phase
1-TMP = 2,4,4-trimethyl-1-pentene
2-TMP = 2,4,4-trimethyl-2-pentene
TMPA = 2,2,4-trimethylpentane
V = vapor phase

Literature Cited

1. Trotta R, Marchionna M, Amoretto F. An iso-octane technology to produce alkylate streams. *Today's Refinery*. 1999;10:21-24.
2. Sanfilippo D. Dehydrogenation of paraffins: Key technology for petrochemicals and fuels. *CATTECH*. 2000;4:56-73.
3. Hunszinger P, Järvelin H, Purola VM, Nurminen M, Khalil MS, Birkhoff R. Start-up and operation of the first on-purpose isooctane unit at Alberta Envirofuels Inc., Edmonton, Canada. Paper AM-03-43. Proc of the NPRA 2003 Annual Meeting, San Antonio, TX, Mar. 23–25; 2003.
4. Sarkar A. *A Catalytic Distillation Process for One-step Production of Isooctane from Isobutene—Process Development, Modeling and Analysis*. PhD Thesis. Waterloo, Ontario, Canada: University of Waterloo; 2005.
5. Ng FTT, Rempel GL. Catalytic distillation. In: Horváth IT, ed. *Encyclopedia of Catalysis*. Vol. 2. New York, NY: Wiley–Interscience, 2003:477-509.
6. Lylykangas MS, Rautanen PA, Krause AOI. Liquid-phase hydrogenation kinetics of isooctenes on Ni/Al_2O_3. *AIChE J*. 2003;49:1508-1515.
7. Lylykangas MS, Rautanen PA, Krause AOI. Liquid-phase hydrogenation kinetics of isooctenes on Co/SiO_2. *Appl Catal A Gen*. 2004a;259: 73-81.
8. Lylykangas MS, Rautanen PA, Krause AOI. Hydrogenation and deactivation kinetics in the liquid-phase hydrogenation of isooctenes on Pt/Al_2O_3. *Ind Eng Chem Res*. 2004b;43:1641-1648.
9. Bartholomew CH. Mechanisms of catalyst deactivation. *Appl Catal A Gen*. 2001;212:17-60.
10. Di Gerolamo M, Catani R, Marchionna M. *Process and Catalysts for the Hydrogenation of Branched Olefins Derived from the Dimerization of Isobutene in the Manufacture of High-Octane Fuels*. U.S. Patent Application No. 20030078462 (2003).
11. Ribeiro FH, Wittenau AES, Bartholomew CH, Somorjai GA. Reproducibility of turnover rates in heterogeneous metal catalysis: Compilation of data and guidelines for data analysis. *Catal Rev Sci Eng*. 1997;39:49-76.
12. Augustine RL. *Heterogeneous Catalysis for the Synthetic Chemist*. New York, NY: Marcel Dekker; 1996:345-348.
13. Rylander PN. *Hydrogenation Methods*. New York, NY: Academic Press; 1985:29-34.
14. Augustine RL, Yaghmaie F, Van Peppen JF. Heterogeneous catalysis in organic chemistry. 2. A mechanistic comparison of noble-metal catalysts in olefin hydrogenation. *J Org Chem*. 1984;49:1865-1870.
15. Karinen RS, Lylykangas MS, Krause AOI. Reaction equilibrium in the isomerisation of 2,4,4-trimethylpentenes. *Ind Eng Chem Res*. 2001;40: 1011-1015.
16. Satterfield CN. *Mass Transfer in Heterogeneous Catalysis*. Cambridge, MA: MIT Press; 1970.
17. Gupta AK, Bhattacharyya KK, Saraf SK. Kinetics of liquid-phase hydrogenation of isooctenes over a supported palladium catalyst. *Indian J Technol*. 1985;23:184-189.
18. Satterfield CN. *Heterogeneous Catalysis in Industrial Practice*. New York, NY: McGraw-Hill; 1991.
19. Young CL, ed. *Solubility Data Series: Hydrogen and Deuterium*. Vol. 5/6. New York, NY: Pergamon Press; 1981.
20. Reid RC, Prausnitz JM, Sherwood TK. *The Properties of Gases and Liquids*. 4th Edition. New York, NY: McGraw Hill; 1987.
21. Smith JM, Van Ness HC. *Introduction to Chemical Engineering Thermodynamics*. 4th Edition. New York, NY: McGraw-Hill; 1987:393-395.
22. Prausnitz J, Anderson T, Grens E, Eckert C, Hsieh R, O'Connell J. *Computer Calculations for Multicomponent Vapor–Liquid and Liquid–Liquid Equilibria*. Upper Saddle River, NJ: Prentice Hall; 1980.
23. Horiuti J, Polanyi M. Exchange reactions of hydrogen on metallic catalysts. *Trans Faraday Soc*. 1934;30:1164-1172.
24. Bond GC, Wells PB. The mechanism of the hydrogenation of unsaturated hydrocarbons on transition metal catalysts. In: Eley DD, Weisz PB, Pines H, eds. *Advances in Catalysis and Related Subjects*. Vol. 15. New York, NY: Academic Press; 1964:91-226.
25. Beebe TP, Yates JT. An in situ infrared spectroscopic investigation of the role of ethylidyne in the ethylene hydrogenation reaction on Pd/Al_2O_3. *J Am Chem Soc*. 1986;108:663-671.
26. Neurock M, van Santen RA. A first principle analysis of C–H bond formation in ethylene hydrogenation. *J Phys Chem B*. 2000;104: 11127-11145.
27. Siegel S. Stereochemistry and the mechanism of hydrogenation of unsaturated hydrocarbons. In: Eley DD, Pines H, Weisz PB, eds. *Advances in Catalysis and Related Subjects*. Vol. 16. New York, NY: Academic Press; 1966:123-177.
28. Kiperman SL. Some problems of chemical kinetics in heterogeneous hydrogenation catalysis. In: Červený L, ed. *Catalytic Hydrogenation*. New York, NY: Elsevier; 1986:1-52.
29. Coleman TF, Li Y. On the convergence of reflective Newton methods for large-scale nonlinear minimization subject to bounds. *Math Program*. 1994;67:189-224.
30. Coleman TF, Li Y. An interior, trust region approach for nonlinear minimization subject to bounds. *SIAM J Optim*. 1996;6:418-445.
31. Froment GF, Bischoff KB. *Chemical Reactor Analysis and Design*. 2nd Edition. Toronto, Canada: Wiley; 1990:99-103.
32. Bond GC, Rank JS. The metal-catalyzed hydrogenation of C5 unsaturated hydrocarbons in the liquid phase. In: Sachtler WMH, Schuit GCA, Zweitering P, eds. *Proceedings of the Third International Congress on Catalysis*. Vol. 2. Amsterdam, The Netherlands: North-Holland; 1965:1225-1236.

Appendix: Discretized Model Equations

In the discretized equations, the superscripts denote the time step and the subscripts denote the discretization points. A representative nonuniform grid section is shown in Figure A1. A fully implicit scheme has been adopted. Upon discretization, the following set of equations was obtained:

$$\frac{(n_i^L)^{j+1} - (n_i^L)^j}{\Delta t} + \frac{(n_i^V)^{j+1} - (n_i^V)^j}{\Delta t} = A(D_{eff}^i)^{j+1}\left[\frac{(c_i)_2^{j+1} - (c_i)_1^{j+1}}{\theta_1 \Delta z}\right] \qquad i = 1, \ldots, 5 \quad \text{(A1)}$$

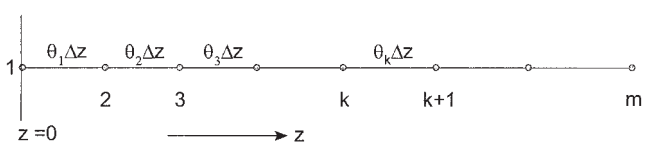

Figure A1. Arrangement of a general numerical grid segment used to solve the simultaneous ODE–PDE system.

At the surface of the catalyst, $z = 0$.

$$\frac{\sum_{i=1}^{6}(n_i^L)^{j+1}}{(\rho^L)^{j+1}} + \frac{\sum_{i=1}^{6}(n_i^V)^{j+1}}{(\rho^V)^{j+1}} = V^R \quad \text{(A2)}$$

$$\left[K_i^{eq}\frac{n_i^L}{\sum_k n_k^L}\right]^{j+1} = \left[\frac{n_i^V}{\sum_k n_k^V}\right]^{j+1} \qquad i = 1, \ldots, 5; \quad k = 1, \ldots, 6 \quad \text{(A3)}$$

$$\left[\frac{n_6^V}{\sum_i n_i^V}\right]^{j+1} = \left[\frac{H}{P^T}\frac{n_6^L}{\sum_i n_i^L}\right]^{j+1} \qquad i = 1, \ldots, 6 \quad \text{(A4)}$$

For discretization point $k = 2, \ldots, (m-2)$

$$\varepsilon_P \frac{(c_i)_k^{j+1} - (c_i)_k^j}{\Delta t} - (D_m^i)_k^{j+1}\frac{2}{(\Delta z)^2}\left[\frac{(c_i)_{k-1}^{j+1} - (c_i)_k^{j+1}}{\theta_{k-1}(\theta_{k-1}+\theta_k)} + \frac{(c_i)_{k+1}^{j+1} - (c_i)_k^{j+1}}{\theta_k(\theta_{k-1}+\theta_k)}\right] = (r_i\rho_S)_k^{j+1} \quad \text{(A5)}$$

where $i = 1, \ldots, 6$ and for discretization point $k = (m-1)$

$$\varepsilon_P \frac{(c_i)_k^{j+1} - (c_i)_k^j}{\Delta t} - (D_m^i)_k^{j+1}\frac{2}{(\Delta z)^2}\left[\frac{(c_i)_{k-1}^{j+1} - (c_i)_k^{j+1}}{\theta_{k-1}(\theta_{k-1}+\theta_k)}\right] = (r_i\rho_S)_k^{j+1} \qquad i = 1, \ldots, 6 \quad \text{(A6)}$$

Manuscript received Apr. 5, 2005, and revision received Sept. 28, 2005.